Surface Science Letters

Growth kinetics in self-assembling monolayers: a unique adsorption mechanism

A. Eberhardt [a,*], P. Fenter [b], P. Eisenberger [c,d]

[a] *Los Alamos National Laboratory, MS G-755, Los Alamos, NM 87545, USA*
[b] *Argonne National Laboratory, ER-203, Argonne, IL 60439, USA*
[c] *Princeton University Physics Department, Princeton, NJ 08544, USA*
[d] *Columbia Earth Institute, New York, NY 10027, USA*

Abstract

The adsorption kinetics of decanethiol ($CH_3(CH_2)_9SH$) self-assembled from vapor on single crystal Au(111) surfaces have been investigated using grazing incidence X-ray diffraction These in situ studies demonstrate the existence of two distinct adsorption mechanisms, including a unique associative mechanism in which the growth rate increases quadratically with the molecular impingement rate These observations indicate that the self-assembly kinetics in these membrane-like films are more complex than previous studies have suggested © 1998 Elsevier Science B V

Keywords Adsorption kinetics; Alkanethiols, Chemisorption, Gold, Mercaptans, Self-assembly; X-ray scattering, diffraction, and reflection

Self-assembled monolayers (SAMs) have been intensively studied as one of the simplest and most immediately useful of the self-organizing organic systems [1–4]. They offer an ideal model for fundamental studies of organic/inorganic interfaces, cell membranes, and complex chemisorption systems. They also have technical relevance in many areas, such as corrosion inhibition, adhesion control, nano-fabrication, molecular recognition, and bio-sensors [5,6]. Consequently, SAMs have been extensively characterized by most available surface science techniques, including microscopy, diffraction, spectroscopy, and wetting, with the aim of better understanding their structure and dynamics

and for the more practical purpose of creating organic devices [7]. As a result, the saturation coverage structure of decanethiol on Au(111) is well understood, consisting of a close-packed, commensurate, rectangular $C(4\sqrt{3} \times 2\sqrt{3})R30°$ (abbreviated $C(4 \times 2)$) unit mesh containing four molecules [8–13] A lower density $11 \times \sqrt{3}$ (striped) phase has also been reported, and is believed to correspond to a structure in which the molecules lie down with the hydrocarbon chains parallel to the surface [9–12]. At elevated temperatures the system disorders and enters a melted state in which the molecules are mobile [13].

Although many studies have focused on the structures and chemical properties of these saturation coverage SAMs, few have considered the self-assembly process itself. Several previous studies of

* Corresponding author Fax (+1) 505 667 8021, e-mail ariane@lanl gov

monolayer growth from solution at room temperature have found that the molecules adsorb with first-order Langmuir kinetics [14–18], although one has seen a different functional form [19]. A recent vapor deposition scanning tunneling microscopy study additionally examined the dynamics of monolayer formation under one particular growth condition [20]. However, in order to determine the underlying physics of the self-assembly process, the kinetics of monolayer formation must be understood in greater detail. The fundamental processes involved in self-assembly are studied here by examining the growth mechanisms from the vapor phase over a broad range of temperatures and impingement rates, utilizing in situ grazing incidence X-ray diffraction (GIXD).

All measurements were taken at the Exxon X10B beamline at the National Synchrotron Light Source, Brookhaven National Laboratories. The studies were performed in an ultra-high vacuum chamber (5×10^{-9} Torr base pressure) mounted on a Huber four-circle diffractometer. Before deposition the single-crystal gold substrate was cleaned with repeated sputter–anneal cycles. Cleanliness and surface order were confirmed by observation of the $22 \times \sqrt{3}$ gold surface reconstruction. A calibrated leak valve was used to maintain a vapor pressure in the range of 10^{-7} to 10^{-5} Torr of decanethiol during monolayer growth. The ion gage used to measure this pressure was estimated to be a factor of 8.0 more sensitive to decanethiol vapor than to nitrogen (derived from Ref. [21]). All filaments were turned off during the growth to avoid contamination. The sample temperature was controlled with an external water supply. The decanethiol was received from Aesar with a nominal purity of 97%, and volatile impurities were removed by repeated pumping cycles for several hours before use. The final purity of the decanethiol utilized in the growth measurements was found to be better than 99% [22], and companion samples grown from still higher purity distilled molecules showed identical behavior.

Fig. 1 illustrates a scan through the first-order diffraction peak indicated, a signal characteristic of the C(4×2) structure [8]. Since the integrated
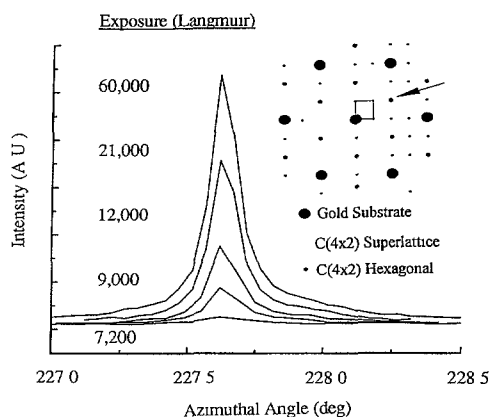

Fig 1 Diffraction peaks A representative series of scans through a diffraction peak arising from the C(4×2) structure is shown [8] These data were taken at 30°C and an impingement rate of 5 9/L s The inset, a schematic of the 2D diffraction pattern, indicates the darker hexagonal peak at $(q_x, q_y, q_z) = (1\ 25, 0\ 725, 0\ 8)\ \text{Å}^{-1}$, used for the growth studies owing to its relatively high intensity The integrated intensity, the area under the curves fit with a Lorentzian line shape, is directly proportional to the number of molecules in this particular phase This area is shown at each point of the growth curves in Fig. 2 The error bars were left off of this illustration for greater clarity, but are reflected in the error bars of Fig. 2.

intensity of a diffraction peak is proportional to the number of molecules in the structure, the scattering intensity relative to saturation is directly proportional to the coverage of that phase, irrespective of the average domain size or degree of order in the system. This total intensity is also independent of the structural details of the particular monolayer phase examined (In particular, the interpretation of this signal in terms of coverage does not depend on the presence or absence of sulfur dimers, as have been inferred by a previous crystallographic analysis of this system [8].) The integrated intensity at each point was measured by scanning through the peak as indicated in Fig. 1, then fitting the curve with a Lorentzian line shape to measure the total area under each curve. The time evolution of the total intensity under the peak at a fixed molecular impingement rate is illustrated in Fig. 2, which displays two representative growth curves of the increase in the C(4×2) diffraction intensity as a function of time. These curves have similar shapes characterized by an initial period in which no signal is observed, fol-
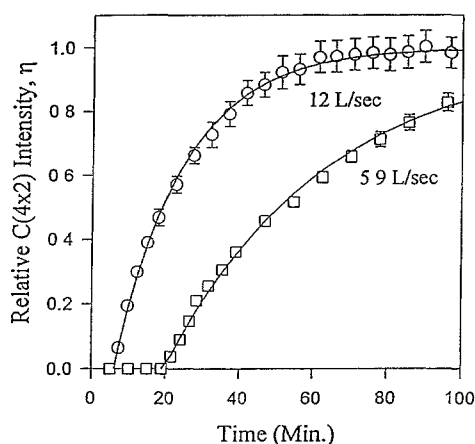
Fig 2. Growth curves Two representative vapor-deposited growth curves are shown at 30°C, measuring the integrated diffraction intensity as a function of deposition time at two impingement rates (in units of langmuir per second) The curves shown measure scattering intensity of the C(4×2) structure only, initially the monolayer is in another phase, as implied by the delay in signal onset The solid lines are a fit to Eq (2), and the rates thus derived are utilized in the curves of Fig 3

lowed by an asymptotic approach to saturation. This suggests a growth model in which the deposition rate is described by first-order Langmuir kinetics, where the rate of growth is proportional to the number of available sites:

$$\frac{d\theta}{dt} = R(1-\theta), \quad \theta = 1 - e^{-Rt}, \tag{1}$$

where θ is the fractional monolayer coverage and R the chemisorption rate. As other studies have shown, the bare gold surface is initially covered by a lower density striped phase, which does not contribute to this C(4×2) Bragg peak [9–11,20]. Diffraction in this phase is thus observed only above a critical coverage at time t_c when islands of denser C(4×2) nucleate within a completed monolayer of striped phase. During the growth of the C(4×2) islands, the surface remains completely covered by a combination of C(4×2) and striped phases [20]. Phenomenologically, the C(4×2) evolution can therefore be described as Langmuir growth with a time offset [23]·

$$\eta = 1 - e^{R(t-t_c)} \quad \text{for } t > t_c \tag{2}$$

where η is the C(4×2) coverage, shown in the fit

in Fig. 2. Within this scenario, the measured rate R explicitly refers to the total chemisorption rate of decanethiol during the growth of the C(4×2) phase, taking into account the existence of a full monolayer of the less dense striped phase [23], and depends on the product of the impingement rate P and sticking coefficient S:

$$R = P \times S. \tag{3}$$

The kinetic behavior in the latter part of the growth process is thus quantified here, although more work is needed to explore the initial low coverage regime. Previous studies have also suggested the existence of long-term reorganization processes, a third time regime, involving a reordering of the hydrocarbon chains [14–17]. Although the measurements shown here are sensitive to this type of reordering, no such process was observed, possibly due to the relatively short hydrocarbon chain length utilized in these studies.

The effects of temperature and molecular impingement rate on monolayer growth rate are illustrated in Fig. 3, which indicates two distinct growth processes. At high temperatures and low impingement rates the growth rate increases linearly with impingement rate as might be expected. This is fundamentally due to an adsorption process in which the molecules incident on the surface adsorb or desorb independently of each other and of the overall impingement rate, as is reflected in the common utilization of the Langmuir as a unit of exposure (1 L = 10^{-6} Torr s). In contrast to this simple behavior, at low temperatures and high impingement rate, the growth rate increases *quadratically* with thiol impingement rate. Any non-linear scaling of growth with impingement rates immediately suggests a cooperative adsorption process, in which more than one molecule is required for adsorption, the total needed expressed by the scaling power. As the non-linear process in this case has a quadratic dependence, a bimolecular process is implied. It is important to note that in all regimes, the growth curves from which the sticking coefficient is extracted (illustrated in Fig. 2), still have a simple Langmuir form. This implies that the growth rate is not affected by nucleation or substrate effects. The difference is only that in the low temperature regime, the stick-
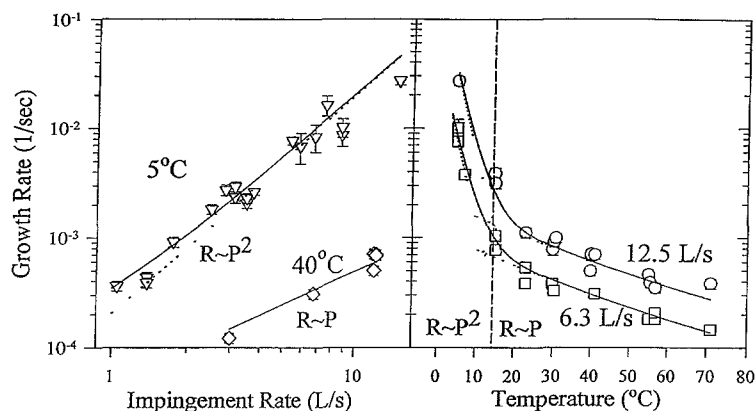
Fig 3 Temperature and impingement rate dependence of growth rate The chemisorption rate is indicated as a function of impingement rate at two representative temperatures in the left panel. At 40°C the dependence is linear, but at 5°C the growth rate increases *quadratically* with the impingement rate at high pressures. The variation with temperature of the two-component growth rate at two fixed impingement rates is shown in the right panel The solid lines are the fit to Eq (4) This is the sum of the two different processes, each of which is shown as a dashed line The transition point indicating the dominance of a particular growth process is clearly visible in both lines of the right panel, and shifts with the change in impingement rate

ing coefficient *S*, defined in Eq. (3), is no longer independent of impingement rate. This scaling is not an artifact of the method used for extracting rates from growth curves, as the same effect can be seen simply by scaling the time axes in order to overlay the growth curves at a given temperature and plotting the required scale factors.

Further evidence for two distinct growth processes is found in an examination of the temperature dependence of the growth rate. Each regime, linear and quadratic, shows a distinct exponential decrease in rate with increasing temperature (Fig. 3, right panel), implying that adsorption proceeds via a physisorbed precursor state to chemisorption [24]. As the chemisorption of each thiol molecule requires the release of a single hydrogen atom, it seems reasonable to suggest that the quadratic adsorption process is related to a bimolecular reaction whose rate-limiting step is the formation of molecular hydrogen. Consequently, these kinetic results are not necessarily related to the final equilibrium structure of the completed monolayer [8].

It is also apparent from the temperature dependence, particularly the existence of a transition region and the domination of the faster process in each regime, that the two processes operate in parallel, as opposed to one complex growth mode

with two different rate-limiting steps. The overall rate of monolayer formation with two growth mechanisms can therefore be written:

$$R = \frac{d\theta}{dt} = PS(T, P) = A_1 P\, e^{E_1/kT} + A_2 P^2\, e^{E_2/kT} \quad (4)$$

in which *R* refers to the measured rate in Eq. (2). This simple expression has been found to explain the growth rates spanning a broad range of impingement rates (0.2–20 L s^{-1}), growth rates (8 × 10^{-4}–3 × 10^{-2} s^{-1}), and substrates temperatures (5–70°C) [23], of which representative data are indicated in Fig. 3. As both the temperature and impingement rate dependencies of the two processes are different, regimes in which one or the other process dominates can be accessed by altering either the substrate temperature or the molecular impingement rates, as shown in the two sections of Fig. 3. An empirical fit to the full data set results in the following values, shown as the solid lines of that figure:

$$E_1 = 0.30 \pm 0.05 \text{ eV}$$

and

$$E_2 = 2\,1 \pm 0.2 \text{ eV}.$$

In order to understand these energy barriers from

a more fundamental perspective, the individual adsorption, desorption, and interaction processes must be incorporated into elementary rate equations. While this is beyond the scope of this paper, the simplified equation shown here reproduces the demonstrated growth behavior, including both the linear and quadratic adsorption processes. The details will be presented elsewhere, but the formalism reveals that E_1 refers to the difference between the barriers to chemisorption and desorption for an individual decanethiol molecule trapped in a physisorption precursor state, whereas E_2 has a more complex form involving these barriers as well as molecular interaction energies [23,25].

In both the linear and quadratic regimes of Fig. 3, the temperature dependence indicates an exponential decrease in adsorption rate with increasing temperature. This is strong evidence for a physisorbed precursor to chemisorption [24]. A qualitative picture of the adsorption process can be inferred. The surface is initially covered by a completed striped phase [9–11,20]. Subsequent adsorption results in the formation of islands in the C(4×2) phase, although there is no preferential adsorption near island edges, implying the possibility of lateral diffusion during or after the adsorption process. As the physisorbed population itself depends linearly on the impingement rate, a pairing of molecules in either this precursor state or during the adsorption process gives rise to a quadratic dependence on the impingement rate at low temperatures and high pressures. At high temperatures and low pressures, the molecules simply adsorb individually, but still through a physisorbed precursor, and always with the Langmuir form expressed in Eq. (2).

These studies indicate that even this comparatively simple and very well studied system exhibits an unexpectedly high degree of complexity not apparent from previous work, including the observation of the unique bimolecular adsorption mechanism described here for the first time. This provides a new context for growth studies at a molecular level, and underlines the necessity for further work to understand the early stages of monolayer growth, as well as the effect of the equilibrium structural phase behavior on the growth kinetics. The high degree of complexity in

this "simple" system suggests that such behavior may be typical for this class of materials, with its numerous internal degrees of freedom and competing interactions.

Acknowledgements

References

[1] R G Nuzzo, D L Allara, J Am Chem Soc 105 (1983) 4481
[2] N. Camillone, III, C E D Chidsey, G -Y Liu, G Scoles, J Chem Phys 98 (1993) 3503
[3] G E Poirier, M J. Tarlov, Langmuir 10 (1994) 2853
[4] R G Nuzzo, B R Zegarski, L H Dubois, J Am Chem Soc 109 (1987) 733
[5] L H Dubois, R G Nuzzo, Annu Rev Phys Chem 43 (1992) 437
[6] A Kumar. H.A Biebuyck, G M Whitesides, Langmuir 10 (1994) 1498
[7] A Ulman, An Introduction to Ultrathin Organic Films: From Langmuir–Blodgett to Self-Assembly, Academic Press, Boston, 1991.
[8] P Fenter, A. Eberhardt, P Eisenberger, Science 266 (1994) 1216
[9] N Camillone, III, T Y B Leung, G Scoles, SPIE Proc., LASE vol 2125, 1994.
[10] N Camillone, III, T Y B Leung, P Schwartz, P Eisenberger, G Scoles, Langmuir, in press
[11] N Camillone, III et al , J Chem Phys 101 (1994) 11031
[12] G E. Poirier, M.J Tarlov, H E Rushmeier, Langmuir 10 (1994) 3383
[13] P Fenter, P Eisenberger, K S Liang, Phys Rev Lett 70 (1993) 2447
[14] C D Bain et al., J Am Chem Soc 111 (1989) 321
[15] M Buck et al , J Vac Sci Technol. A 10 (1992) 926
[16] G Hahner, Ch Woll, M Buck, M Grunze, Langmuir 9 (1993) 1955

[17] D S Karpovich, G J Blanchard, Langmuir 10 (1994) 3315

[18] R C Thomas, L Sun, R M Crooks, Langmuir 7 (1991) 620

[19] K A Peterlinz, R. Georgiadis, Langmuir 12 (1996) 4731.

[20] G E Poirier, E D Pylant, Science 272 (1996) 1145

[21] R L Summers, NASA technical note TND-5285

[22] T Y B Leung, personal communication of G C mass spectroscopy measurement.

[23] A S Eberhardt, Ph D Thesis, Princeton University, 1997

[24] W H Weinberg, in. M. Grunze, H J Kreuzer (Eds), Kinetics of Interface Reactions. Springer, Berlin, 1987.

[25] A Eberhardt, T Y B Leung, F Schreiber, P. Fenter, P Eisenberger, in preparation